

# Magnetic Properties of Fe Ions in a Silicate Glass and Ceramic

A. MEKKI<sup>1)</sup>

*Department of Physics, King Fahd University of Petroleum & Minerals,  
Dhahran 31261, Saudi Arabia*

(Received by J. I. B. Wilson August 3, 2000; in revised form December 4, 2000;  
accepted December 6, 2000)

Subject classification: 75.40.Cx; 75.50.Ee; 75.50.Kj; S10.15

A homogeneous glass with composition  $0.60\text{SiO}_2-0.3\text{Na}_2\text{O}-0.10\text{Fe}_2\text{O}_3$  was prepared and devitrified to produce a glass ceramic having a single crystalline phase of formula  $\text{Na}_5\text{Fe}(\text{SiO}_3)_4$ . The dc magnetic susceptibility measurements performed on the glass and the heat-treated sample have shown that the magnetic exchange interaction is antiferromagnetic and of equal strength in both samples investigated. It was shown that  $M$  versus  $H$  data at different temperatures do not collapse to a single curve in the  $M$  versus  $H/T$  representation for both the glass and the heat-treated sample, further indicating an antiferromagnetic interaction in both materials. The  $M$  versus  $H$  data for the glass sample was fitted with Brillouin function by keeping the total number of magnetic ions constant and varying the proportion of ferrous ions until a best fit was achieved. The  $[\text{Fe}^{2+}]/[\text{Fe}_{\text{total}}]$  concentration ratio obtained from the fit is in good agreement with the value obtained from X-ray photoelectron spectroscopy (XPS) performed on the glass sample.

## 1. Introduction

Magnetic properties of amorphous materials containing transition metal ions have been extensively studied in the past for both practical and fundamental reasons [1–6]. Oxide glasses, specifically those containing  $\text{Fe}_2\text{O}_3$ , have been the subject of numerous publications due to their interesting magnetic, structural, and optical properties [7–11]. However, little work has focused on a comparative study of the magnetic properties of the glass and the glass ceramic obtained by heat treatment of the parent glass.

The glass composition we have investigated in the present work is part of a series of sodium iron silicate glasses, namely  $(0.70-x)\text{SiO}_2-0.30\text{Na}_2\text{O}-x\text{Fe}_2\text{O}_3$ , where  $x = 0, 0.05, 0.10, 0.15,$  and  $0.20$ , that has been studied by means of X-ray photoelectron spectroscopy (XPS) [12]. From the O 1s spectra, we were able to determine the bridging to non-bridging oxygen ratio. It was also found that  $\text{Fe}^{2+}$  and  $\text{Fe}^{3+}$  ions exist simultaneously in these glasses. The Fe 3p core level spectra were deconvoluted with two contributions, one from  $\text{Fe}^{2+}$  ions and the other from  $\text{Fe}^{3+}$  ions, and the number of ferric and ferrous ions for each glass composition were obtained. It was found that  $\text{Fe}^{2+}$  was the preferred valence state of iron for low  $x$  values, while  $\text{Fe}^{3+}$  is predominant at high  $\text{Fe}_2\text{O}_3$  content. Other physical properties of these glasses have been measured, such as thermal expansion and density.

In the present study, we report the measurements of the magnetization and the dc magnetic susceptibility for the  $x = 0.1$   $\text{Fe}_2\text{O}_3$  glass and the glass ceramic obtained by heat treatment of the parent glass at its crystallization temperature determined by dif-

---

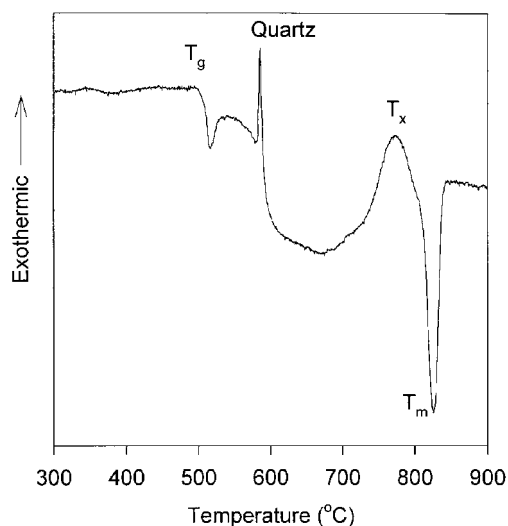
<sup>1)</sup> Phone: +966 3 860 4292; Fax: +966 3 860 2293; e-mail: akmekki@kfupm.edu.sa

ferential thermal analysis (DTA). A similar study has been done for the  $x = 0.05$  glass composition and the results have been published elsewhere [13].

The objective of the present study is to compare the magnetic properties of the sodium silicate glass and the crystallized samples with composition  $x = 0.10$ . We will calculate, from the inverse magnetic susceptibility versus temperature data, two parameters: the paramagnetic Curie temperature,  $\theta_p$ , and the effective magnetic moment,  $\mu_B$ , which will give us qualitative information about the strength of the magnetic interaction. From the  $M$  versus  $H$  data of the glass samples, we will also calculate the number of ferric and ferrous ions, by fitting the experimental data to Brillouin function and we will compare the relative amounts obtained from this analysis with those obtained from XPS.

## 2. Experimental Details

The glass composition prepared had the formula  $0.60\text{SiO}_2-0.30\text{Na}_2\text{O}-0.10\text{Fe}_2\text{O}_3$ . Analytical grade powders of  $\text{Fe}_2\text{O}_3$ ,  $\text{Na}_2\text{CO}_3$  (for  $\text{Na}_2\text{O}$ ), and  $\text{SiO}_2$ , in the required stoichiometric ratios, were melted in a platinum crucible at  $1300^\circ\text{C}$  for two hours. The melt was cast into preshaped graphite-coated steel molds yielding glass rod specimens (for XPS analysis) which were annealed,  $50^\circ\text{C}$  below the glass transition temperature ( $T_g$ , determined by DTA) for two hours, then slowly cooled to room temperature. A rod was crushed into fine powder, which was used for various other measurements. The chemical composition of the glass samples was determined by inductively coupled plasma spectroscopy (ICP). Each glass composition was analyzed at least twice and the estimated relative uncertainty in the ICP technique is about 5%. The analysis led to the following composition;  $0.618\text{SiO}_2-0.298\text{Na}_2\text{O}-0.085\text{Fe}_2\text{O}_3$  [12]. Differential thermal analysis (DTA) was performed at a heating rate of  $10^\circ\text{C}/\text{min}$  using a Stanton Redcroft 673-4 instrument. Quartz was used as a reference material since its  $\alpha \rightarrow \beta$  transition helps establish the exo/endothemic directions and the transformation occurs at a known temperature ( $573 \pm 0.5^\circ\text{C}$ ), thus confirming the accuracy of the temperature



scale of the DTA trace. The glass was then heat-treated at the crystallization temperature, determined from the DTA trace shown in Fig. 1, for six hours, with heating rate of  $1^\circ\text{C}/\text{min}$  and cooling rate of  $5^\circ\text{C}/\text{min}$ . The X-ray diffraction patterns (XRD), for the glass and the crystallized sample, were obtained using  $\text{Cu K}_\alpha$  radiation and a standard Phillips diffractometer, alignment of the system

Fig. 1. DTA trace of the glass sample showing the different transformation temperatures. Quartz was used as the reference material

being checked against a silicon polycrystalline standard. The magnetization data ( $M$  versus  $H$  and  $M$  versus  $T$ ) were recorded using a computer controlled PAR/Lakeshore 4500/150A variable temperature vibrating sample magnetometer (VSM) incorporating a 9 T superconducting magnet and a temperature controller, capable of temperature control in the range 2 to 300 K. The temperature measuring sensor was a calibrated carbon glass resistor located near the specimen. The system was calibrated using pure nickel standard. The overall accuracy in the temperature measurements is better than  $\pm 1\%$  throughout the range, while that of the magnetization measurements is estimated to be approximately  $\pm 5\%$ . The XPS experimental details and analysis are given in Ref. [12].

### 3. Results and Discussion

Figure 1 shows the DTA curve of the as quenched sample. Two exothermic peaks and an endothermic peak are observed. The first exothermic peak, sharp and narrow, is due to the  $\alpha \rightarrow \beta$  transition of  $\text{SiO}_2$ , which was used as the standard material. This event occurs at a known temperature of  $573 \pm 0.5^\circ\text{C}$ . The second exothermic peak, small and broad, is due to the crystallization of the glass. An endothermic event occurs just after the crystallization peak and is indicative of the melting of the crystal phase formed during the crystallization process. Another feature at around  $500^\circ\text{C}$  is observed in the DTA trace. This feature represents the glass transition temperature  $T_g$ . The glass transition temperature, the crystallization temperature and the melting temperature of the glass sample were found to be  $T_g = 505 \pm 1^\circ\text{C}$ ,  $T_x = 775 \pm 1^\circ\text{C}$  and  $T_m = 826 \pm 1^\circ\text{C}$ , respectively.

The glass sample has been heat-treated at the crystallization temperature at heating and cooling rates of  $1^\circ\text{C}/\text{min}$  and  $5^\circ\text{C}/\text{min}$ , respectively. The glass ceramic obtained has been analyzed by X-ray diffraction. The XRD powder patterns of the glass and the heat-treated sample are shown in Fig. 2 in the range  $2\theta = 10^\circ$  to  $70^\circ$ . It was found that there is a single crystalline phase in the heat-treated sample (Fig. 2b) and this phase was identified as  $\text{Na}_5\text{Fe}(\text{SiO}_3)_4$ . This has also been checked from the phase diagram of  $\text{SiO}_2\text{-Na}_2\text{O-Fe}_2\text{O}_3$  [14]. Two small peaks are seen in the XRD pattern of the glass sample at  $2\theta = 38^\circ$  and  $45^\circ$  (Fig. 2a). These peaks arise from the aluminum sample holder.

The inverse dc magnetic susceptibility ( $\chi^{-1}$ ) data for the glass and the heat-treated sample are shown in Fig. 3. The data has been measured in the temperature range 2.5–60 K. The magnetic susceptibility is expressed in

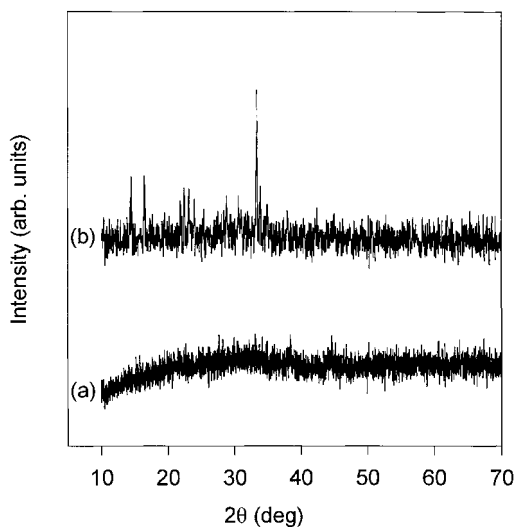


Fig. 2. XRD patterns for a) the glass and b) the heat-treated sample

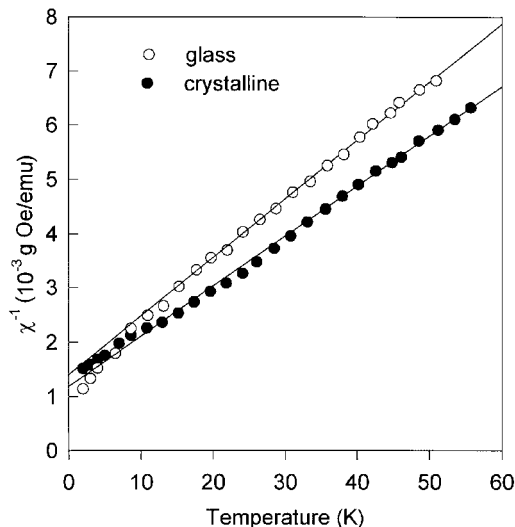


Fig. 3. The inverse magnetic susceptibility versus temperature for the glass and the heat-treated sample. The solid lines correspond to the Curie-Weiss law

emu/g Oe. For the glass and the heat-treated sample, the high temperature susceptibility follows a Curie-Weiss behavior:  $\chi = C/(T-\theta_p)$  with an antiferromagnetic Curie temperature. The downward curvature of the inverse susceptibility plot at low temperature, seen in the glass sample (Fig. 3), has been theoretically explained by Simpson [15]. The Simpson model assumes that the random nature of the glass matrix allows a fraction of the transition metal ions to be 'shielded' from the exchange interaction with another metal ion.

These shielded ions give rise to paramagnetic behavior, which tends to dominate the susceptibility at low temperatures. Similar behavior has been seen in iron phosphate, manganese phosphate [4], and in iron borate glasses [5]. The low temperature inverse susceptibility behavior of the crystallized sample is different from that of the glass sample and characteristic of a normal antiferromagnet with an upward curvature at low temperatures. The onset of the curvature occurs at a temperature called 'Neel temperature',  $(T_N) \approx 12$  K. The relevant data obtained from the magnetic susceptibility measurements are reported in Table 1 for the glass and the crystalline sample. The Curie temperature is a rough measure of the strength of the interaction between the magnetic ions in the sample, with a higher value implying a stronger interaction and/or more ions participating in the interaction. When comparing the magnetic properties of the crystalline sample and the parent glass, we see almost no change in both  $\theta_p$  and  $\mu_{\text{eff}}$ . This would indicate that Fe ions behave magnetically in a similar way whether the environment is glassy or crystalline for this  $\text{Fe}_2\text{O}_3$  content in the glass. However, in the case of  $x = 0.05$   $\text{Fe}_2\text{O}_3$  doped glass and crystalline sample, the situation is different [13]. It was found that the magnetic exchange interaction is antiferromagnetic in both samples and much stronger in the crystalline sample than in the glass sample. This would indicate that the magnetic exchange interaction in the crystalline and the parent glass depends strongly on the Fe content in the glass.

Table 1

Magnetic parameters determined from the  $\chi^{-1}$  vs.  $T$  data for the glass and the crystalline sample. The total number of Fe ions is determined from ICP with an uncertainty of  $\pm 5\%$

sample	[Fe ions] ( $10^{20}/\text{g}$ )	$C$ ( $10^{-3}$ emu K/g)	$\theta_p \pm 1$ ( $^{\circ}\text{C}$ )	$\mu_{\text{eff}} \pm 0.2$ ( $\mu_B$ )
glass	14.7	9.6	11	5.6
crystalline	14.7	10.6	14	5.7

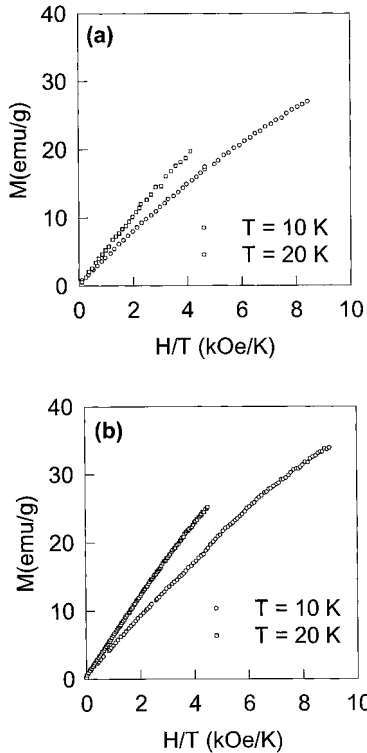


Fig. 4. The magnetization data of a) the glass sample and b) the heat-treated sample taken at two different temperatures and plotted against the reduced variable  $H/T$

The effect of the exchange interaction can be graphically seen by plotting  $M$  versus  $H/T$  at different temperatures. This is done for the glass and the heat-treated sample and the data are shown in Fig. 4 for two temperatures ( $T = 10$  K and  $T = 20$  K). We see that the data do not collapse to a single curve, indicating an antiferromagnetic interaction in both samples. However, in the case of silicate glasses doped with various amounts of CuO [16], it was found that the data on the  $H/T$  scale collapsed completely to a single curve, indicating that copper in the glass structure behaves paramagnetically. We also note that the spread of the  $M$  versus  $H/T$  data in both samples is similar, indicating that the magnetic exchange interaction in both sample is of nearly equal magnitude. It is to be noted that in the case of 0.05  $Fe_2O_3$  doped glass, the magnetic behavior of Fe ions in the heat-treated and parent glass samples is different [13]. It was found that the spread of the magnetic data on the  $H/T$  scale was

larger in the heat-treated sample, indicating a stronger antiferromagnetic interaction in that sample. One can calculate, quantitatively, the strength of the exchange interaction but it will not be considered here because it is beyond the scope of the present work.

Data on similar systems support the small antiferromagnetic coupling found in these materials [17].

The field dependence of the magnetization of the glass is shown in Fig. 5 for the glass sample. The  $M$  vs.  $H$  data curves toward the field axis for low temperatures ( $T \leq 10$  K) and becomes linear for higher tem-

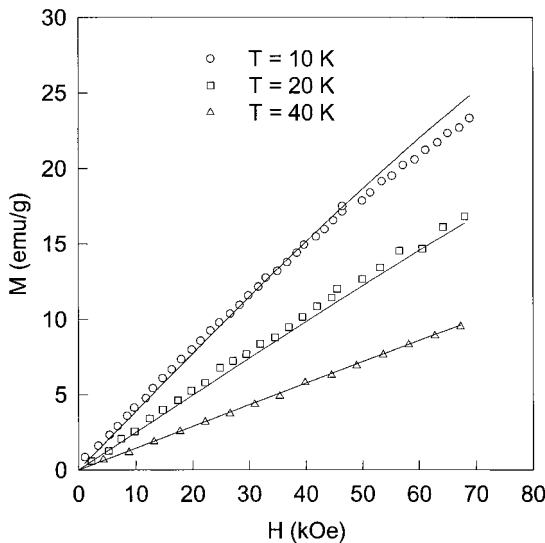


Fig. 5. Magnetization versus magnetic field for the glass sample at different temperatures. The experimental data are shown by points, while the solid lines represent the fits to the data

peratures. The magnetization of the glass increases as the temperature is lowered to 10 K. We tried to fit the magnetization data with the following equation:

$$M = NgJ\mu_B B_J(x) \quad (1)$$

where  $B_J(x) = [(2J + 1)/2J] \coth [(2J + 1)x/2J] - (1/2J) \coth (x/2J)$  is the Brillouin function,  $M$  is the magnetization,  $N$  is the number of magnetic ions and  $x = gJ\mu_B H / [k_B(T - \theta_p)]$ , the rest of the symbols have the usual meaning, with  $g = 2$ , and  $\theta_p$  takes the values reported in Table 1.

In our case the magnetization for the glass sample was fitted to equation (1) with two terms – a contribution from  $\text{Fe}^{2+}$  ions ( $J_1 = 2$ ) and another from  $\text{Fe}^{3+}$  ions ( $J_2 = 5/2$ ) as follows:

$$M_{\text{total}} = M(\text{Fe}^{2+}) + M(\text{Fe}^{3+}) = N_1 g J_1 \mu_B B_{J_1}(x_1) + (N - N_1) g J_2 \mu_B B_{J_2}(x_2), \quad (2)$$

where  $N$  is the total number of Fe ions/g of the sample obtained from the ICP analysis. The number  $N_1$  (number of  $\text{Fe}^{2+}$  ions/g of the sample) was used as the adjustable parameter to obtain the best fit to the experimental data. The value of  $J_1$  was taken to be 2 instead of 4 ( $S_1 = 2$  and  $L_1 = 2$ ) due to the fact that transition metals in glasses show spin-only type moments because of the extent of the 3d orbitals which allows a quenching of the orbital angular momentum by interaction with the ligand field [18]. The fitting of the experimental data is shown in Fig. 5 by a solid line for the  $M$  vs.  $H$  data taken at three different temperatures. Good agreement was obtained, which is shown by the solid lines in the figure, except at 10 K where deviation can be observed, which may be explained by the existence of pair-wise Fe–Fe interaction, which is dominating at low temperature. The number of  $\text{Fe}^{2+}$ ,  $\text{Fe}^{3+}$  ions and the ratio  $[\text{Fe}^{2+}]/[\text{Fe}_{\text{total}}]$  obtained from the fits are shown in Table 2. This data is compared to the one deduced from XPS measurements in which the concentrations of  $\text{Fe}^{2+}$  and  $\text{Fe}^{3+}$  were obtained from the deconvolution of the Fe 3p spectrum. The ratio  $[\text{Fe}^{2+}]/[\text{Fe}_{\text{total}}]$  was found to be equal 23% [12]. It is to be noted that XPS is a surface analytical technique, while the magnetic measurement is a bulk technique. The agreement between the two techniques might be due to the fact that in the XPS analysis, the sample was fractured in ultra high vacuum (UHV) as explained in Ref. [12]. This would imply that a fractured sample in UHV is the best surface to be studied and representing the bulk state.

An attempt has been made to heat-treat a glass rod (6 mm in diameter, 2 cm in length) for XPS analysis to obtain information on the valence state of iron after crystallization for a comparison with the glass. An SEM image of the heat-treated rod revealed that there was surface crystallization with the center of the rod being still glassy. Further XPS analysis of a fully crystallized sample rod is under consideration in our laboratory.

Table 2

Concentrations of  $\text{Fe}^{2+}$  and  $\text{Fe}^{3+}$  needed to fit the  $M$  vs.  $H$  data at different temperatures for the glass sample

$T$ (K)	$[\text{Fe}^{2+}]$ ( $10^{20}/\text{g}$ )	$[\text{Fe}^{3+}]$ ( $10^{20}/\text{g}$ )	$[\text{Fe}^{2+}]/[\text{Fe}_{\text{total}}]$
10	4.4	10.3	0.29
20	3.4	11.3	0.23
40	4.7	10	0.31

#### 4. Conclusion

We have produced a crystalline sample (glass ceramic) by heat treating a glass sample having the nominal composition  $0.60\text{SiO}_2-0.30\text{Na}_2\text{O}-0.10\text{Fe}_2\text{O}_3$ . A single phase identified as  $\text{Na}_5\text{Fe}(\text{SiO}_3)_4$  was formed after heat treatment of the parent glass. We have then made a comparative study of the type of magnetic interaction of Fe ions in the glass and the heat-treated sample. The magnetic exchange interaction was found to be of nearly equal strength in both samples. The number of  $\text{Fe}^{2+}$  ions obtained from the fit to the  $M$  versus  $H$  data for the glass sample is in good agreement with the XPS findings.

**Acknowledgement** The author would like to acknowledge the support of King Fahd University of Petroleum and Minerals.

#### References

- [1] C.H. PERRY, D.L. KINSER, L.K. WILSON, and J.G. VAUGHN, *J. Appl. Phys.* **50**, 1601 (1979).
- [2] E.J. FREIBELE and N.C. KOON, *Solid State Commun.* **14**, 1247 (1974).
- [3] E.J. FREIBELE, N.C. KOON, L.K. WILSON, and D.L. KINSER, *J. Am. Ceram. Soc.* **57**, 237 (1974).
- [4] T. EGAMI, O.A. SACHI, A.W. SIMPSON, A.L. TERRY, and F.A. WEDGWOOD, in: *Amorphous Magnetism, Proc. Internat. Symp. on Amorphous Magnetism*, Eds. H.O. HOOPER and A.M. GRAFF, Plenum Press, New York 1973.
- [5] M.A. VALENTE and S.K. MANDIRATTA, *Phys. Chem. Glasses* **33**, 149 (1992).
- [6] S.K. MANDIRATTA, M.A. VALENTE, and J.A. PERNBOOM, *J. Non-Cryst. Solids* **134**, 100 (1990).
- [7] W.J. BLACKBURN and B.P. TILLY, *J. Mater. Sci.* **9**, 1265 (1974).
- [8] H. LAVILLE and J.C. BERNIER, *J. Mag. Magn. Mater.* **15-18**, 193 (1980).
- [9] F. SCHUMACHER, K.A. HEMPEL, and F. VON STAAB, *J. Physique* **49**, C8-949 (1988).
- [10] H. LAVILLE and J.C. BERNIER, *Solid State Commun.* **27**, 259 (1978).
- [11] C. CHAUMONT and J.C. BERNIER, *J. Solid State Chem.* **38**, 246 (1981).
- [12] A. MEKKI, D. HOLLAND, C.F. McCONVILLE, and M. SALIM, *J. Non-Cryst. Solids* **208**, 267 (1996).
- [13] A. MEKKI and KH. A. ZIQ, *J. Mag. Magn. Mater.* **189**, 207 (1998).
- [14] N.L. BOWEN, J.F. SCHAIRER, and H.W. WILLEMS, *Am. J. Sci.*, 5th Ser. **20**, 419 (1930).
- [15] A.W. SIMPSON and J.M. LUCAS, *J. Appl. Phys.* **42**, 2181 (1971).
- [16] A. MEKKI, D. HOLLAND, KH. A. ZIQ, and C.F. McCONVILLE, *Phys. Chem. Glasses* **39**, 45 (1998).
- [17] S.K. ASADOV, E.A. ZAVADSKII, V.I. KAMEVEN, K.V. KAMENEV, and B.M. TODRIS, *Physica B* **182**, 167 (1992).
- [18] G. CALAS, *Spectroscopic methods in mineralogy and geology*, in: *Review in Mineralogy*, Vol. 18, Ed. F.C. HAWTHORNE, Mineralogical Society of America, Washington, D.C., 1988.

